Associative electron detachment: $O^- + H \rightarrow OH + e^-$

Prabhat K. Acharya, Rick A. Kendall, and Jack Simons
Department of Chemistry, University of Utah, Salt Lake City, Utah 84112

(Received 11 June 1985; accepted 3 July 1985)

Associative electron detachment processes are important experimental events that can readily be modeled using modern theoretical methods. Experimental methods to date have only allowed one to obtain the relative vibrational distribution of the neutral product molecules. Using a non-Born–Oppenheimer, nonadiabatic, viewpoint that utilizes a fully *ab initio* approach, we are able to obtain absolute rates ($\sim 10^4$ s for the $O^- + H$ system) for transitions from an initial state specified by collision energy and impact parameter, to specific vibrational and rotational states of the neutral OH and a detached electron. The fact that these rates are slow for the $O^- + H$ system is due to the large electron affinity of OH (1.8 eV). These rates have an obtuse propensity favoring vibrationally and rotationally hot products. This propensity arises from contributions that are independent and dependent of the angular momentum of the system, an aspect that is of substantial experimental interest. A detailed study of $O^- + H \rightarrow OH(V', J') + e^-$ is given and generalizations for detachment processes in other systems ($F^- + H$, LiH^-, NH^-, BH^-) are made.

I. INTRODUCTION

Diatomic associative electron detachment[1] (AED) involves the ejection of an electron when an atomic anion (e.g., F^- or O^-) and another atom (e.g., H, D, or Br) collisionally associate to produce a neutral diatomic molecule in a vibration-rotation state labeled V', J'. For example,

$$O^- + H \rightarrow OH(^2\Pi, V', J') + e^- \tag{1a}$$

or

$$F^- + D \rightarrow FD(^1\Sigma, V', J') + e^-. \tag{1b}$$

In some sense, the AED process can be viewed as the reverse of the dissociative electron attachment (DEA) event

$$e^- + AB \rightarrow A^- + B, \tag{2}$$

however, the electronic states and mechanisms of the two processes are, in fact, often not the same.

Consider, e.g., the $O^-(^2P) + H(^2S) \rightarrow OH(^2\Pi, V', J') + e^-$ AED event. The above two states of O^- and H give rise to a bound $^1\Sigma$ potential energy curve and a repulsive $^1\Pi$ state (see Fig. 1); the former describes the ground electronic state of OH^- and has a $\pi^4\sigma^2$ configuration whereas the latter correlates with a singlet-coupled configuration of the form $\pi^3\sigma^2\sigma^*$. The $^1\Sigma$ state of OH^- lies below the ground $^2\Pi$ state of OH (which has a $\pi^3\sigma^2$ configuration near its equilibrium bond length) at all bond lengths. However, the repulsive $^1\Pi$ OH^- state crosses the $^2\Pi$ state of OH. AED at low collision energies occurs when O^- and H collide on the $^1\Sigma$ surface and eject an electron to produce $^2\Pi$ OH in some V', J' state. Although it is true, according to microscopic reversibility, that an electron could attach a π-orbital of $^2\Pi$ OH to yield OH^- $^1\Sigma$ above its dissociation threshold, thereby generating $O^- + H$, such a process is not commonly viewed as DEA. Conventional DEA would involve attachment of an electron to the σ^* orbital of OH to produce $^1\Pi$ OH^- which subsequently dissociates to produce O^- and H. The essential difference between the above two processes (which involve electron attachment to π and σ^* orbitals, respectively) is that the former (reverse-AED) is electronically exoergic whereas the latter (DEA) is electronically endoergic.

Furthermore, the reverse-AED process requires dynamical coupling[2] with the vibration-rotation degrees of freedom; DEA can occur without such coupling. That is, within the Born–Oppenheimer separation, which neglects dynamical couplings, the DEA process can occur because there are bond lengths R where the $^1\Pi$ state of OH^- lies above $^2\Pi$ state of OH. Hence the kinetic energy of the incident electron can be converted into electronic energy (in attaching to the σ^* orbital) thus producing $^1\Pi$ OH^- at that R. In contrast, in reverse-AED there exists no bond length at which $^1\Sigma$ OH^- lies above $^2\Pi$ OH. Therefore, the kinetic energy of the incident electron cannot be absorbed within the electronic degrees of freedom at any R. The vibration-rotation degrees of freedom must become involved, in which case $OH(^2\Pi, V', J') + e^- \rightarrow OH^-(^1\Sigma, V, J)$ can occur if the OH^- gains vibration-rotation energy at the expense of the incident electron's kinetic energy.

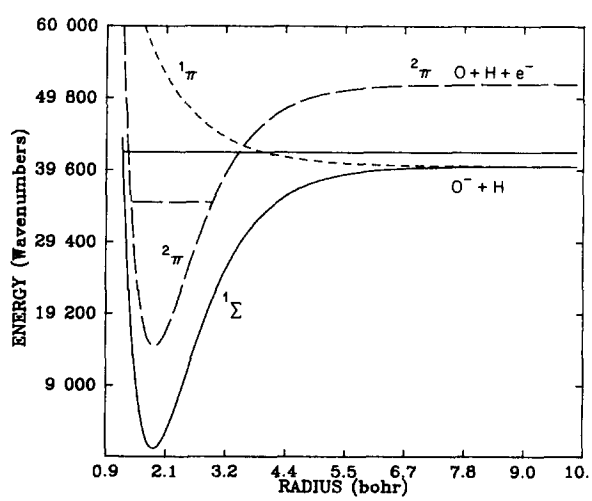

FIG. 1. OH^- and OH potential energy curves ($J = 0$).

 0021-9606/85/203888-06$02.10

There do exist AED events which do not involve dynamical coupling but which arise because the relevant anion and neutral potential energy curves cross. For example, in $F^- + H \rightarrow HF(V', J') + e^-$, the $^2\Sigma$ HF^- and $^1\Sigma$ HF potential energy curves cross near the equilibrium bond length of HF (see Fig. 2). Thus, in F^-, H collisions, the electron ejection can occur without electronic-vibration rotation coupling whenever the HF internuclear distance moves within the value of R at which the curves cross.

In the present work, attention is restricted to the AED process in the particular $O^- + H$ case which requires nonadiabatic or dynamical coupling, because it is of immediate interest[3] to researchers in Leone's laboratory. Neither reverse-AED nor DEA are treated here. The experimentalists are interested in several aspects of the $O^- + H$ AED process which can be addressed via theoretical simulation: the absolute rates of electron ejection, the branching ratios for the formation of $OH(^2\Pi, V', J')$ in various vibration-rotation levels (V', J'), and a physical understanding of the observed internal-state propensities. These are the goals of the present paper.

The *ab initio* theoretical calculations undertaken in our laboratory involve three steps:

(1) Using methods described in earlier publications[2] and summarized in Sec. II to compute absolute state-to-state electron ejection rates.

(2) Averaging over the initial states appropriate to the distributions of collisional energies (E) and impact parameters (b) or angular momenta (J) which characterize the experiment.

(3) Summing contributions over final states which cannot be experimentally resolved (e.g., the angle of ejection of the electron). In the following section these steps are described in some detail.

II. ELECTRON EJECTION RATE CALCULATIONS

A. Rate expression

In an earlier publication[2a] we demonstrated how to obtain the rate of electron ejection from a bound vibration-rotation state of a diatomic anion such as OH^- (V, J) to produce a bound state of the corresponding neutral such as OH (V', J'). The same state-to-state rate expression can be used for AED by replacing the anion's bound vibration-rotation wave function $\chi_{V,J}(R,\theta,\phi)$ by an appropriate scattering function $\chi_{E,J}(R,\theta,\phi)$ describing the relative translation of the two species (e.g., O^- and H) having collision energy E and collisional angular momentum $J(J+1)\hbar^2$. Since it is experimentally impossible to specify the collisional angular momentum (or equivalently, the impact parameter b), we must multiply the state specific rate by $P(J)$, the normalized probability weighting for realizing an initial value of J, and by $P(E)$, the probability of realizing a collision energy E. We must then integrate over dJ and dE to obtain the initial-condition-average rate for production of OH in $V'J'$. Therefore, the working rate expression is as follows:

$$Rate = \sum_J \int dE P(J) P(E) \frac{2\pi h^3}{\mu^2} \rho |\chi^*_{V',J'} \times \int \Psi^{0*} \nabla \Psi^- \mathbf{dr} \cdot \nabla \chi_{E,J} \, \mathbf{d}R \, |^2. \quad (3)$$

Ψ^0 is the electronic wave function of the combined OH plus continuum electron system, Ψ^- is the electronic wave function of the OH^- anion, and $\chi_{E,J}$ is the $O^- + H$ scattering function discussed above. The gradient operator ∇ acts with respect to the coordinates R, θ, ϕ describing the relative radial and angular the coordinates of the oxygen and hydrogen nuclei. The density of translational states of the ejected electron is denoted by ρ.

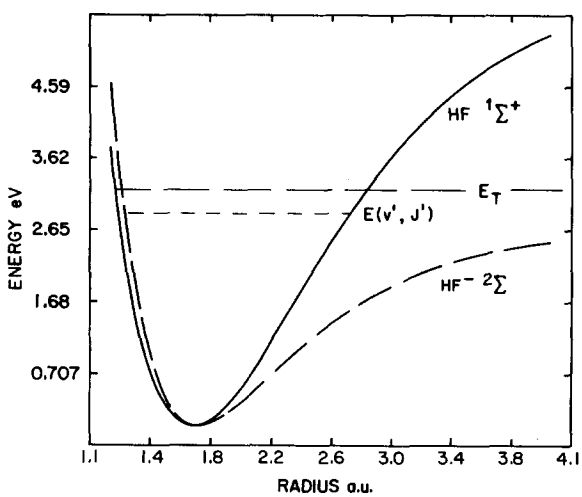

FIG. 2. HF^- and HF potential energy curves ($J = 0$).

B. Calculations of ingredients in rate expression

The anion's electronic wave function Ψ^- is approximated as a single Slater determinant consisting of the Hartree–Fock orbitals of the $^1\Sigma$ $1\sigma^2 2\sigma^2 3\sigma^2 1\pi^4$ configuration. The particular choice of Gaussian-type orbital (GTO) basis set is described in Ref. 2(b). The neutral-plus-free electron wave function Ψ^0 is also taken to be a single Slater determinant $1\sigma^2 2\sigma^2 3\sigma^2 1\pi^3 \phi_k$ containing the same $1\sigma, 2\sigma, 3\sigma$, and 1π orbitals as were used in Ψ^- and a continuum orbital ϕ_k of the orthogonalized-plane-wave type. The derivative $\nabla\Psi^-$ is formed by analytically differentiating the GTO's and differentiating numerically interpolated values of the molecular orbital linear expansion coefficients appearing in Ψ^- as described in Ref. 2(b). Although these Koopmans' theorem descriptions of Ψ^0 and $\nabla\Psi^-$ represent lowest order approximations, their use for OH^- and OH is reasonably justified as discussed in Ref. 2(b).

The nuclear motion wave functions $\chi_{E,J}$ and $\chi_{V',J'}$ are products of spherical harmonics and radial wave functions $F_{E,J}$ and $F_{V',J'}$ which are obtained by numerically integrating the appropriate radial Schrödinger equations. To obtain $F_{E,J}$ the effective radial potential is taken to be the $^1\Sigma$ OH^- potential given in Ref. 2(b) plus a centrifugal potential $\hbar^2 J(J+1)/2\mu R^2$ due to the collisional angular momentum of the O^- and H. The $F_{V',J'}$ are calculated by numerically integrating the radial Schrödinger equation in which the centrifugal potential appropriate to J' and the $^2\Pi$ OH potential energy curve constitute the effective potential. The OH^- and OH potential energy curves were approximated as

Morse potentials whose parameters are given in Ref. 2(b).

Calculation of the orthogonalized plane wave ϕ_k makes use of the energy difference $E-\epsilon(V',J')$ which is the O^- and H collision energy minus the OH (V',J') vibration rotation energy. This is, of course, the kinetic energy of the ejected electron. For the AED events considered here, the de Broglie wavelengths of the OPW function are in the 10–100 Å range. Further details concerning how ϕ_k is orthogonalized to the occupied orbitals of OH^- are given in Ref. 2(b).

C. Initial-condition weighting factors

For a given O^- plus H asymptotic kinetic energy E, there exists a value of J above which the barrier in the angular momentum effective potential (see Fig. 3) exceeds E; such a value of J is referred to as $J_M(E)$. Collisions with angular momenta (or impact parameters $b\sim\hbar\sqrt{J(J+1)/2\mu E}$) greater than J_M do not sample regions of internuclear distance where the OH^- potential energy is strongly attractive and where $\nabla\Psi^-$ is most substantial. Such collisions are then not effective in bringing about AED. For this reason, when averaging over all possible values for the initial collisional angular momentum or impact parameter, values of J substantially above J_M can be ignored.

The probability weighting factor $P(J)dJ$ appropriate to the collisional angular momentum is easily obtained from geometrical arguments involving the impact parameter b. For a given value of b, all collisions on a disk of radius b and thickness db are equally likely. This disk has area $2\pi bdb$. Converting $2\pi bdb$ to angular momentum involves using the relation given above and results in a weighting factor of $\hbar^2\pi(2J+1)\,dJ/2\mu E$. Normalizing this between $J=0$ and $J=J_M$ gives

$$P(J)dJ=(2J+1)dJ/J_M(J_M+1),\quad J\leqslant J_M \tag{4}$$

which shows that collisions having larger J values or impact parameters are more heavily weighted (however, beyond J_M the weighting is effectively zero).

The corresponding weighting factor for the collisional energy distribution cannot simply be obtained from geometrical or statistical arguments; it depends upon how the experiment is carried out. In the simulations performed here, it was assumed that the appropriate distribution of relative kinetic energies $(1/2\,\mu v^2)$ can be described in terms of a Maxwell–Boltzmann distribution characterized by a temperature T:

$$P(v)dv=4\pi(\mu/2\pi kT)^{3/2}v^2\exp(-\mu v^2/2kT)dv\,. \tag{5}$$

In terms of the collision energy $E=1/2\,\mu v^2$, this normalized probability distribution reduces to

$$P(E)dE=(2/\sqrt{\pi})(kT)^{-3/2}\sqrt{E}\,\exp(-E/kT)dE. \tag{6}$$

This distribution has an average energy

$$\bar{E}=\int P(E)E\,dE=3/2\,kT, \tag{7a}$$

and a second moment

$$\sqrt{E^2-(\bar{E})^2}=\sqrt{3/2}kT=0.83\,\bar{E}. \tag{7b}$$

In principle, the state-specific rate should be calculated at many values of E, weighted by $P(E)dE$ of Eq. (6), and followed by integration over E. In the simulations presented here, we chose to compute the rates at discrete values of E (66, 256, and 732 cm^{-1}) all of which lie within the range of collision energies characterizing the Leone experiments.[1]

D. Vibration and rotation dependence of ejection rates

The rate expression shown in Eq. (3) contains dependences on the final vibrational quantum number V' and the final rotational quantum number J' which merit further remarks. The angular integrals in Eq. (3) involve integrations over products of spherical harmonics of the form

$$Y^*_{J'M'}\,\frac{1}{\sin\theta}\,\frac{dY_{JM}}{d\theta}\sin\theta\,d\theta\,d\phi$$

and

$$Y^*_{J'M'}\,\frac{1}{\sin^2\theta}\,\frac{dY_{JM}}{d\phi}\sin\theta\,d\theta\,d\phi,$$

both of which arise from angular derivatives $\nabla\Psi^-$, as well as $Y^*_{J'M'}Y_{JM}\sin\theta\,d\phi\,d\theta$ which associate with the radial derivatives in $\nabla\Psi^-$. Each of these angular integrals can be shown to be either independent of J or to vary with J as a low power of $(2J+1)$. Hence, the rate expression contains J-independent pieces as well as terms which vary as $(2J+1)$, $(2J+1)^2$, etc. The J-independent factors originate from the radial derivatives in $\nabla\Psi^-$ whereas those which depend on $(2J+1)^n$ arise from angular derivatives in $\nabla\Psi^-$. We refer to these rate contributions on vibrational and rotational terms, respectively.

Furthermore, those integrals for which the final angular momentum differs significantly from the initial contribute little to the overall rate. That is, because the ejected electron can carry away little momentum or angular momentum, the change in the angular momentum of the nuclei is small.[1] For this reason, we consider only the dominant $J=J'$ terms in our simulations.

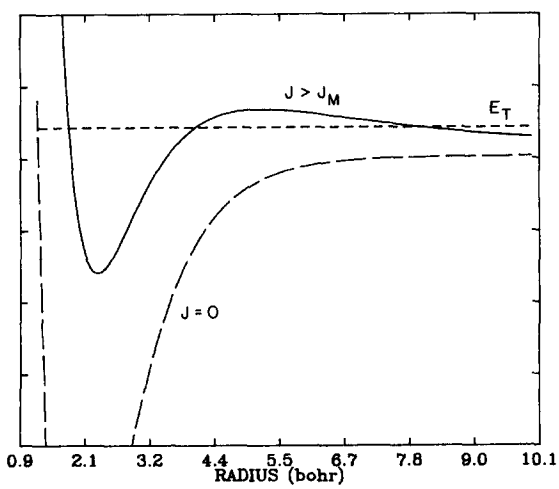

FIG. 3. Illustrative potential energy curves for $J=0$ and for $J>J_M$. The value of J_M depends upon the collision energy E_T.

III. RESULTS

In Tables I–IV are displayed the state-to-state electron ejection rates for the O^- + H AED process. Several features

TABLE I. Total vibration-rotation induced rates (s^{-1}) at a collision energy of 66 cm^{-1}.

$J=$	$V'=8$	7	6	5	4	3	2	1	0
0	0.113	68.8	125	61.1	12.5	0.975	0.008	0.003	0.001
3	7.62	449	971	515	116	10.9	0.230	0.007	0.003
5	23.0	541	1570	935	231	24.9	0.799	0.001	0.004
7	...	288	1590	1140	321	40.5	1.83	0.004	0.002
10	...	0.051	1440	1680	616	101	6.89	0.011	0.000

of this data merit attention. First, the fastest state-specific absolute rate is of the order of $10^3\ s^{-1}$; at a collision frequency of approximately 10^{13} coll s^{-1}, this translates into a rate of 10^{-10} per collision. Even the total rate of production of electrons (i.e., the sum over all state-specific rates) does not exceed $3\times10^4\ s^{-1}$. We therefore conclude that AED in $O^- + H$ will provide very little experimental signal and is probably not a good candidate for further experimental study. It is our opinion that the very large detachment energy ($\approx$1.8 eV) of OH^- is the primary cause of these slow absolute rates; it simply takes a long time to convert 1.8 eV of vibration-rotation energy into electronic energy.

The propensities for producing OH in various vibrational levels (averaged over J) shown in Table IV shown interesting trends. Transitions to very low V' values are not favored because of phase cancellation in the Franck–Condon-like integrals over R which appear in Eq. (3). Transitions to higher V' values are favored, but by no means do we observe transitions primarily into only one vibrational level. Moreover, transitions to the highest accessible V' values do not occur as rapidly as those to vibrational levels which are slightly lower in energy. The origins of these somewhat unusual vibrational propensities lie in the anharmonicities of the OH^- and OH potential curves and in the fact that Eq. (3) involves integration of $\chi^*_{V',J'}\nabla\chi_{EJ}$ which contains both conventional Franck–Condon terms $F^*_{V',J'}F_{EJ}$ and terms arising from the ∇ operator $F^*_{V',J'}(dF_{EJ}/dR)$. The latter terms, in particular, would be expected to connect radial wave functions whose nodal patterns differ by one node. This may be the reason for the small rates of production of OH in the highest accessible V' levels. Quite frankly, the fact that the AED dynamics samples very anharmonic regions of the OH^- and OH potential surfaces and the appearance of $\nabla\chi_{EJ}$ in Eq. (3) combine to yield a vibrational propensity pattern which is not straightforward to fully understand, although there are clear trends that favor high V' values.

The rotation state-specific rates also provide important information about the $O^- + H$ AED dynamics. As discussed in Sec. II D, the rate expression of Eq. (3) contains both J-independent (vibrational) and J-dependent (rotational) terms. The former arises from the radial derivative ∇ whereas the latter came from angular derivatives in ∇. The J-dependence of the state-specific rate is therefore expected to be [see Eq. (3)] of the form $|A + B(2J+1) + C(2J+1)^2 + \cdots|^2(2J+1)$, where the final $(2J+1)$ comes from the $2\pi bdb$ weighting factor. The magnitudes and signs of the A, B, C, etc. factors depend on the integrals involving the radial (A) and angular (B, C, etc.) derivatives.

For all three collision energies and for essentially all vibrational states V', one notices the same interesting trend in the rates as a function of J. The rates start out small for low J, they initially increase as J increases [due largely to the $2\pi bdb$ or $(2J+1)$ weighting factor], then they decrease until just before $J\approx J_M$ is reached at which time they again increase until they are precipitously cut off of $J>J_M$. As noted above, the initial rise in rates is due largely to the $(2J+1)$ weighting factor. The rate decrease at intermediate J values occurs because the A and B factors (see above) are of opposite sign; as J increases, a point is reached where

TABLE II. Total vibration-rotation induced rates (s^{-1}) at a collision energy of 256 cm^{-1}.

$J=$	$V'=8$	7	6	5	4	3	2	1	0
0	0.0287	59.6	93.3	42.7	8.33	0.614	0.0036	0.0023	0.0004
3	1.99	393	714	354	76.1	6.84	0.125	0.0006	0.0020
5	17.2	482	1130	624	148	15.3	0.447	0.0019	0.0025
7	...	323	1320	882	237	28.9	1.24	0.0013	0.0020
10	...	9.87	1190	1250	436	68.8	4.54	0.0675	0.0005
11	...	14.8	1040	1370	533	92.1	6.86	0.142	0.0001
13	...	331	416	1290	678	144	13.7	0.455	0.0014
15	...	...	3.40	988	820	227	27.0	1.26	0.0124
17	...	...	256	170	380	150	23.2	1.45	0.0250

TABLE III. Total vibration-rotation induced rates (s^{-1}) at a collision energy of 732 cm^{-1}.

$J=$	$V'=8$	7	6	5	4	3	2	1	0
0	2.17	56.9	65.7	26.3	4.62	0.291	0.0004	0.0019	0.0003
3	4.97	392	509	220	42.8	3.41	0.0406	0.0059	0.0014
5	0.0883	524	821	391	83.7	7.78	0.176	0.0033	0.0017
7	...	502	1100	601	145	15.9	0.565	0.0000	0.0017
10	...	128	1160	928	289	41.4	2.45	0.0263	0.0006
11	...	15.7	986	989	344	55.1	3.77	0.0645	0.0002
13	...	112	614	1090	489	95.0	8.25	0.242	0.0004
15	...	476	96.4	919	607	150	16.6	0.714	0.0057
17	...	...	142	468	634	216	30.7	1.78	0.0275
18	...	...	548	228	602	251	40.8	2.70	0.0514
21	...	...	...	375	162	261	74.5	7.62	0.242
23	...	...	...	1910	22.6	152	88.3	13.0	0.561
25	...	...	...	...	1050	4.43	74.9	20.0	1.23

$[A + B(2J+1) + \cdots]^2$ becomes small. At such J values, the vibrational (A) and rotational (B, C, etc.) contributions are destructively interfering with one another. As J further increases, the rotational contributions to the rate begin to dominate and so the rate again rises (nonlinearly with J) until, once J_M is exceeded, collisions with even larger J values (impact parameters) no longer have the ability to cause AED.

IV. DISCUSSION

The *ab initio* theoretical simulations whose results are given in Sec. III indicate (a) that AED in $O^- + H$ is so slow ($\sim 10^4\ s^{-1}$) that it is likely to be inaccessible to present experimental observation, (b) that propensity for producing OH in high vibrational levels does occur but the propensity is not sharp due largely to anharmonicity in the OH^- and OH potentials, (c) that vibrational and rotational contributions to the J-state-specific rates engage in destructive interference to yield rotational state populations which rise, then fall, then rise rapidly again (and nonlinearly) with increasing J.

The data obtained in this study of $O^- + H$ AED when combined with our earlier data on purely vibrational (i.e., $J=0$) electron detachment in LiH^- and OH^- allow us to speculate about rates of electron ejection in other anions. Along these lines, we offer the following generalizations:

(1) Anions with large electron detachment energies such as OH^- (1.8 eV) should undergo rather slow (10–$10^5\ s^{-1}$) electron ejection. Anions with small detachment energies such as LiH^-, BH^-, and NH^- should detach more readily[3] (10^8–$10^{11}\ s^{-1}$).

(2) The relative importance of vibrational and rotational motion in causing electron ejection depends upon the nature of the orbital out of what the electron detaches. Orbitals such as the nonbonding 3σ orbital of LiH^- and the antibonding $1\pi_g$ orbital of O_2^- are strongly effected (in energy and radial size) by changes in bond length (i.e., vibration). In contrast, the nonbonding π orbitals of OH^-, NH^-, and BH^- do not vary greatly with bond length; they are, however, strongly effected by rotation of the diatomic bond axis. For these species, rotational motion is expected to be important and the nonlinear J-dependence described above should follow.

(3) AED tends to produce vibrationally and rotationally hot neutrals for reasons given above.

(4) Where rotational motion contributes strongly to the detachment rate, there should exist strong J-dependence in the state-specific rates and λ-doublet levels should display significant rate differences. For example, in $OH^-(^1\Sigma, J) \rightarrow OH(^2\pi, J') + e^-$ the OH should be produced in one component of the λ doublet in greater quantity than the other. In $NH^-(^3\Sigma, J) \rightarrow NH(^2\pi, J') + e^-$ one component of the NH^- λ doublet should detach faster than the other.[3]

TABLE IV. Total vibration-rotation induced rates (s^{-1}) for transitions into specific V' states.

Collision energy (cm^{-1})	$V'=8$	7	6	5	4	3	2	1	0
66	30.7	1350	5700	4330	1300	178	9.76	0.026	0.010
256	19.2	1610	6160	6970	3320	734	77.1	3.38	0.046
732	7.23	2310	6040	8150	4480	1250	341	46.2	2.12

ACKNOWLEDGMENTS

The authors wish to acknowledge the financial support of the National Science Foundation (Grant No. 8206845). We also wish to acknowledge the Harris Corporation for their generous computer system grant.

[1](a) J. C. Weisshaar, T. S. Zwier, and S. R. Leone, J. Chem. Phys. **75**, 4873 (1981); (b) T. S. Zwier, J. C. Weisshaar, and S. R. Leone, *ibid.* **75**, 4885 (1981); (c) J. L. Mauer and J. Schulz, Phys. Rev. A **7**, 593 (1973); (d) V. M. Bierbaum, G. B. Ellison, J. H. Futrell, and S. R. Leone, J. Chem. Phys. **67**, 2375 (1977); (e) M. A. Smith and S. R. Leone, *ibid.* **78**, 1325 (1983); (f) T. S. Zwier, M. M. Maricq, C. J. S. M. Simpson, V. M. Bierbaum, G. B. Ellison, and S. R. Leone, Phys. Rev. Lett. **44**, 1050 (1980).

[2](a) J. Simons, J. Am. Chem. Soc. **103**, 3971 (1981); (b) P. K. Acharya, R. A. Kendall, and J. Simons, *ibid.* **106**, 3402 (1984); (c) P. Acharya, R. Kendall, and J. Simons, Symp. At. Surf. Phys. **84**, 1 (1984).

[3]D. Neumark and W. C. Lineberger have reported large differential rates of electron detachment for the two components of λ doublets in the NH^- ($v = 1$) (private communication). They also report a strong J dependence for one of the λ doublet's rates (indicating strong rotational contributions as discussed in Sec. III) and a weak J dependence of the other λ doublet's rates (indicating dominance of vibrational effects).